Eur. Phys. J. D **46**, 37–39 (2008)
DOI: 10.1140/epjd/e2007-00297-y

THE EUROPEAN PHYSICAL JOURNAL D

Measurement of M-shell X-ray production cross sections for the element $73 \leqslant Z \leqslant 83$ using 5.96 keV photons

A. Küçükönder, Ö. Söğüt[a], C. Dozen, and B.G. Durdu

Kahraman Maraş Sutcu Imam University, Faculty of Science and Arts, Department of Physics, 46100 K. Maraş, Turkey

Received 7 February 2007 / Received in final form 23 May 2007
Published online 24 October 2007 – © EDP Sciences, Società Italiana di Fisica, Springer-Verlag 2007

Abstract. Total M-shell X-ray production cross sections (M XRF) of the some elements in the atomic number range $73 \leqslant Z \leqslant 83$ were measured at 5.96 keV incident photon energy using a Si(Li) detector. The results are compared with the experimental and theoretical values in the literature.

PACS. 32.30.Rj X-ray spectra – 32.80.Cy Atomic scattering, cross sections, and form factors; Compton scattering

1 Introduction

Information regarding the experimental value of X-ray fluorescence (XRF) cross sections for different elements at various photoionization energies is important because of its wide use in the fields of atomic, molecular and radiation physics and non-destructive elemental analysis of materials using XRF techniques [1]. Since various M-shell X-ray lines are not resolved by the available Si(Li) X-ray spectrometer due to its limited resolution, we have measured total M X-ray production cross sections in targets Ta, W, Re, Pt, Au, Pb and Bi by 5.96 keV photons. The energies of incident photons used for photoionization are chosen so that they are below the binding energy of the L shell of elements under investigation. The K- and L-shell electrons are therefore not knocked out and the distribution of M-shell vacancies created by the incident photons is not disturbed due to the shift of vacancies from the K- and L-shells to the M-shell. The restriction on the choice of the energies of the incident photons is useful as it simplifies the calculation of the M-shell X-ray production cross sections needed for comparison with the experimental values. Most of the available experimental data about photon-induced X-ray production cross section and fluorescence yield are limited to K- and L-shells [2–4]. However, measured experimental [5–9,11,12] and theoretical data [10,13–15] on M and higher shells X-ray production cross sections and fluorescence yields in the literature are very spare, due to complexity associated with the M and higher shells X-ray spectrum. The M XRF cross sections for Ta, W, Re, Pt, Au, Pb and Bi at 5.96 keV incident photon energy were reported by Shatendra et al. [11]. They compared their results with the theoretical estimates for Ta only, as they could not obtain theoretical estimates for other elements [1]. The theoretical total M XRF cross sections for the elements in the range $73 \leqslant Z \leqslant 83$ at 5.96 keV were also calculated. A comparison of the measured M XRF cross sections with the theoretical estimate is expected to provide a check on physical parameters such as M-shell photoionization cross sections, fluorescence yields, Coster-Kronig transition probabilities and radiative decay rates, which are used to calculate theoretical M XRF cross sections and the average M-shell fluorescence yields [1]. Therefore, only total M-shell fluorescence cross sections have been measured in this work. In this work, the M-shell production cross sections were studied both experimentally and theoretically under present experimental conditions.

2 Experimental

The target samples were excited by using heavily filtered 5.96 keV from a 100 mCi Fe-55 radiative source and X-rays emitted from samples were detected by Si(Li) ($FWHM = 155$ eV at 5.9 keV) detector system. The purity of commercially obtained materials was better than 99%. Powder samples were sieved for 400 mesh and prepared by supporting an mylar film at 34×10^{-3} g cm^{-2} mass thickness. The experimental geometry is shown in Figure 1. Figure 2 shows a typical M X-ray spectrum of Au. The different components of M X-ray peak [M_γ (M_3-N_5), $M_{\xi 2}$ (M_4-N_2), $M_{\xi 1}$ (M_5-N_3), M_β (M_4-N_6), $M_{\alpha 1}$ (M_5-N_7), $M_{\alpha 2}$ (M_5-N_6) and M_m (M_1-N_2, M_2-N_4, M_3-O_{145})] could be identified though not clearly resolved because of the limitation of detector resolution. Hence, the experimental M X-ray production cross sections were calculated by the following equation [16]:

$$\sigma_M^x = \frac{N_M}{I_0 G \varepsilon \beta_M m} \tag{1}$$

[a] e-mail: omer_sogut@yahoo.com

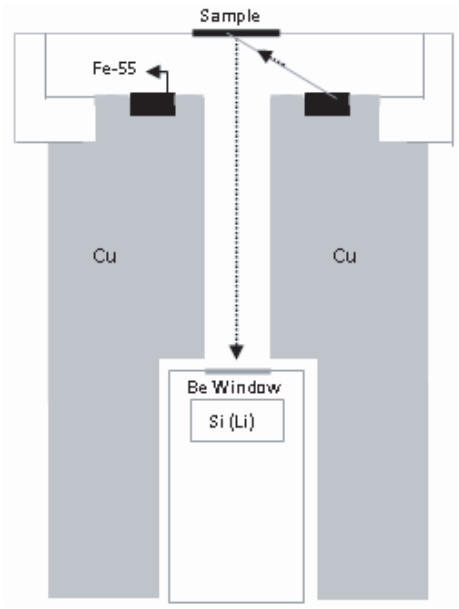

Fig. 1. Experimental setup.

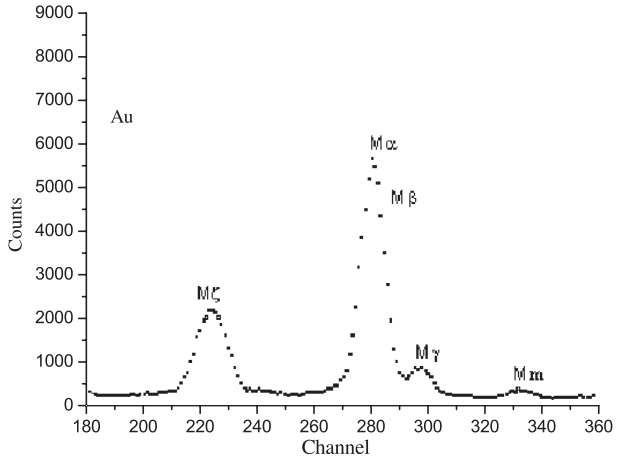

Fig. 2. A typical M X-ray spectrum of Au.

where, N_M is intensity observed for the M X-ray line of the element, ε is the detection efficiency of the detector at the energy of M X-ray, I_0 is the intensity of exciting radiation, m is the mass of the element in sample (g cm^{-2}), G is the geometry factor and β_M is target self absorption correction factor of the target material. The self absorption correction has been calculated by using the following expression obtained by assuming the incidence angle of the fluorescent X-rays subtended at the detector to be approximately 90° [17]

$$\beta_M = \frac{1-\exp[(-1)(\mu_{inc}/\cos\theta_1 + \mu_{emt}/\cos\theta_2)m]}{(\mu_{inc}/\cos\theta_1 + \mu_{emt}/\cos\theta_2)m} \quad (2)$$

where μ_{inc} (cm^2 g^{-1}) and μ_{emt} (cm^2 g^{-1}) [18] are total mass absorption coefficients at the incident photon energy and fluorescent average M X-ray energy of sample, respectively, and m (g cm^{-2}) is the measured mass thickness of sample.

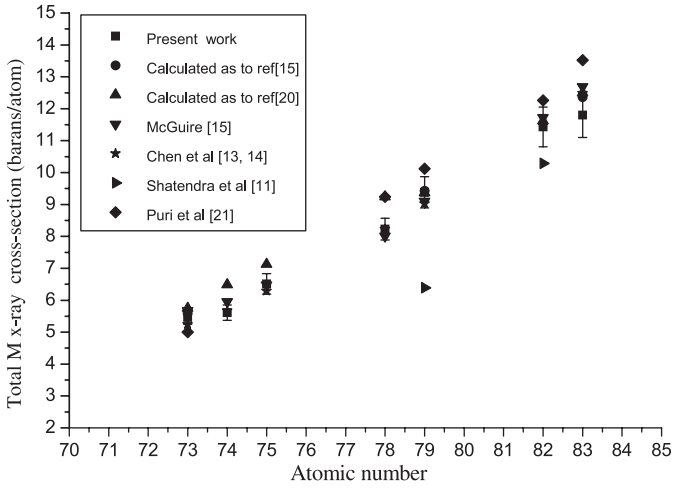

Fig. 3. Comparison of measured, other experimental and theoretical total M-shell X-ray production cross section as a function of atomic number.

In the present work, the product $I_0G\varepsilon$ was determined by measuring the K X-ray yields from Al, Si, Si, P, S, K, Ca, Ti and V in the same geometry. $I_0G\varepsilon$ (detector efficiency) values for the present setup were determined by the following equation [19],

$$I_0G\varepsilon_M = \frac{N_K}{\sigma_K^x \beta_K m} \quad (3)$$

where I_0 is the intensity of exciting radiation falling on the sample, G is the geometry factor, ε_M is the detector efficiency for K X-rays, m is the mass thickness of the sample in g cm^{-2}, N_K is the net count of the corresponding photo peak, β_K is the self-absorption correction factor of the target material, σ_K^x is the K X-ray fluorescence cross section and is given as [19]

$$\sigma_K^x = \sigma_K^P \omega_K \quad (4)$$

where σ_K^P is the K-shell photoionization cross section [20] and ω_K is the K-shell fluorescence yield [21].

3 Theoretical calculations

The experimental values of M XRF cross sections are compared with the calculated values in Table 1 and Figure 3. The theoretical values of the total M XRF cross sections were calculated using the following relationships, given by Gowda and Powers [22]

$$\sigma_{M1}^x = \sigma_{M1}^P \omega_1 \quad (5)$$

$$\sigma_{M2}^x = \left(\sigma_{M1}^P S_{12} + \sigma_{M2}^P\right)\omega_2 \quad (6)$$

$$\sigma_{M3}^x = \left[\sigma_{M1}^P (S_{13} + S_{12}S_{23}) + \sigma_{M2}^P S_{23} + \sigma_{M3}^P\right]\omega_3 \quad (7)$$

$$\sigma_{M4}^x = \left[\sigma_{M1}^P (S_{14} + S_{12}S_{24} + S_{13}S_{34} + S_{12}S_{23}S_{34}) + \sigma_{M2}^P (S_{24} + S_{23}S_{34}) + \sigma_{M3}^P S_{34} + \sigma_{M4}^P\right]\omega_4 \quad (8)$$

Table 1. Comparison of M XRF cross sections of experimental results with other experimental and theoretical results (cm^2 g^{-1}).

Samples	Present work	Calculated as to reference [15]	Calculated as to reference [23]	Fit values	McGuire [15]	Chen et al. [13,14]	Shatendra et al. [11]	Puri et al. [24]
73 Ta	5.46 ± 0.21	5.59	5.75	5.173	5.67	5.24	–	5.00
74 W	5.61 ± 0.24	–	6.49	5.846	5.96	5.67	–	–
75 Re	6.51 ± 0.32	–	7.13	6.519	6.48	6.29	–	–
78 Pt	8.23 ± 0.34	–	9.24	8.538	8.01	8.23	–	9.24
79 Au	9.38 ± 0.49	9.43	9.37	9.211	9.10	9.03	6.39	10.12
82 Pb	11.43 ± 0.62	–	11.62	11.229	11.73	11.48	10.29	12.26
83 Bi	11.80 ± 0.70	12.36	12.5	11.902	12.69	12.49	–	13.52

$$\sigma^x_{M5} = \big[\sigma^P_{M1}(S_{15}+S_{12}S_{25}+S_{13}S_{35}+S_{14}f_{45}+S_{12}S_{23}S_{35} + S_{12}S_{24}f_{45}+S_{13}S_{34}f_{45}+S_{12}S_{23}S_{34}f_{45}) + \sigma^P_{M2}(S_{25}+S_{24}f_{45}+S_{23}S_{35}+S_{23}S_{34}f_{45}) + \sigma^P_{M3}(S_{35}+S_{34}f_{45}) + \sigma^P_{M4}f_{45} + \sigma^P_{M5}\big]\,\omega_5 \quad (9)$$

$$\sigma^x_M = \sum_{i=1-5} \sigma^x_{M_i} \quad (10)$$

where σ^P_{Mi} (i = 1–5) are the M subshell photoionization cross sections [13], ω_i (i = 1–5) are the M subshell fluorescence yields, S_{ij} (i = 1–3, j = 2–5) are the M super Coster-Kronig transition probabilities and f_{45} is the Coster-Kronig transition probability [13–15].

4 Results and discussion

The measured values of total M-shell X-ray production cross sections for the elements Ta, W, Re, Pt, Au, Pb and Bi at 5.96 keV incident energy are listed in Table 1. The experimental results of the M XRF cross sections are compared with other theoretical [13–15,23], experimental [11] and fit values. The errors in our measurements which are due to the counting statistic, the background determination, self absorption correction factor and $I_0 G \varepsilon$ determination are ≈4–6%.

As seen from Table 1, it is evident that the measured values of M XRF cross sections for the elements in the atomic range $73 \leqslant Z \leqslant 83$ differ by 0.5–8% from the theoretical values calculated using ω_i, S_{ij} and f_{45} given by Chen et al. [13,14]. The experimental values differ by 0.4–7% with compare to theoretically calculated values because the theoretical values are calculated using the values of McGuire [15]. Besides, the experimental values differ by 11–46% and 7–13% the experimental values of Shatendra et al. [11] and Puri et al. [8], respectively. Furthermore, the experimental values differ by 0.1–6% with compare to fit values. The experimental cross sections generally agree with the theoretical values (except for the values of Shatendra et al. [11]) and our results are in good agreement with the theoretical values. The discrepancy between the experimental and theoretical values of M XRF cross section may be due to systematic errors in the physical parameters.

As shown in Figure 3, the values of M XRF cross sections increase with the atomic number. The reason for this may be that the binding energy of shell electrons increases with the atomic number (the equation of fit values is $Y(Z) = -43.9475 + 0.67289Z$, $R^2 = 0.99252$, $SD = 0.2498$).

References

1. R.R. Garg, S. Singh, J.S. Shahi, D. Mehta, N. Singh, P.N. Trehan, S. Kumar, M.L. Garg, P.C. Mangal, X-Ray Spectrum. **20**, 91 (1991)
2. R. Durak, Y. Şahin, Phys. Rev. A **57**, 2578 (1998)
3. R. Durak, Y. Özdemir, Spectrochim. Acta B **55**, 177 (2000)
4. R. Durak, Phys. Scripta **58**, 111 (1998)
5. D.V. Rao, R. Cesareo, G.E. Gigante, Nucl. Instr. Meth. B **108**, 227 (1996)
6. K.S. Mann, N. Singh, R. Mittal, K.L. Allawadhi, B.S. Sood, J. Phys. B **23**, 2497 (1990)
7. D.V. Rao, R. Casereo, G.E. Gigante, Radiat. Phys. Chem. **49**, 503 (1997)
8. S. Puri, D. Mehta, B. Chand, N. Singh, P.C. Mangal, P.N. Trehan, Nucl. Instr. Meth. B **73**, 319 (1993)
9. K. Shatendra, K.L. Allawadhi, B.S. Sood, Physica C **124**, 279 (1984)
10. E. Öz, H. Erdoğan, M. Ertuğrul, X-Ray Spectrom. **28**, 198 (1999)
11. K. Shatendra, N. Singh, R. Mittal, K.L. Allawadhi, B.S. Sood, X-Ray Spectrom. **14**, 195 (1985)
12. M. Ertuğrul, E. Traşoğlu, Y. Kurucu, S. Erzeneoğlu, R. Durak, Y. Şahin, Nucl. Instr. Meth. B **108**, 18 (1996)
13. M.H. Chen, B. Craseman, H. Mark, Phys. Rev. A **21**, 449 (1980)
14. M.H. Chen, B. Crasemann, H. Mark, Phys. Rev. A **27**, 2989 (1983)
15. E.J. McGuire, Phys. Rev. A **5**, 1043 (1972)
16. D.V. Rao, R. Cesareo, G.E. Gigante, Radiat. Phys. Chem. **46**, 317 (1995)
17. R.E. Van Grieken, A.A. Markowicz, *Hand Book of X-Ray Spectrometry* (Marcel Dekker Inc., New York, 1993), p. 234
18. J.H. Hubbel, S.M. Seltzer, NISTIR 5632 (1995)
19. W. Bambynek, B. Craseman, R.W. Fink, H.U. Freund, H. Mark, C.D. Swift, R.E. Price, P.V. Rao, Rev. Mod. Phys. **44**, 716 (1972)
20. Scofield, Lawrance Livermore National Laboratory Report No: UCRL 51326 (Unpublished)
21. M.O. Krause, J. Phys. Chem. Ref. Data **8**, 307 (1979)
22. R. Gowda, D. Powers, Phys. Rev. A **31**, 34 (1985)
23. Ö. Sogut, E. Buyukkasap, A. Kucukonder, M. Ertuğrul, O. Dogan, O. Sımsek, X-Ray Spektrom. **31**, 62 (2002)
24. S. Puri, D. Mehta, B. Chand, N. Singh, J.H. Hubbell, P.N. Trehan, Nucl. Instr. Meth. B **73**, 319 (1993)